# Substrate Specificity of the Oncoprotein v-Fps: Site-Specific Mutagenesis of the Putative P+1 Pocket†

Laurel Konkol, T. John Hirai, and Joseph A. Adams*

*Department of Pharmacology, University of California, San Diego, La Jolla, California 92093-0506*

*Received September 8, 1999; Revised Manuscript Received October 25, 1999*

ABSTRACT: Based on the X-ray structure of the insulin receptor kinase [Hubbard, S. R. (1997) *EMBO J. 16*, 5572−5581], Arg-1130 in the oncoprotein v-Fps, a nonreceptor tyrosine protein kinase, is predicted to interact with the P+1 glutamate in substrate peptides. To determine whether this residue is an important recognition element in v-Fps, Arg-1130 was substituted with leucine (R1130L) and glutamic acid (R1130E). The ability of these mutants to phosphorylate the peptide EAEIYXAIE, where X is glutamic acid, alanine, or lysine, was assessed. A comparison of the rates of peptide phosphorylation under limiting substrate concentrations (i.e., $k_{cat}/K_m$ conditions) indicates that substrate specificity is altered by the electrostatic environment of the P+1 pocket. When the pocket displays a positive charge (Arg-1130; wild type), no charge (R1130L), or a negative charge (R1130E), v-Fps prefers to phosphorylate the glutamate peptide over the lysine peptide by a 200:1, 9:1, or 1:1 margin. While $k_{cat}/K_m$ for the glutamate peptide is 50-fold higher for wild type compared to R1130E, $k_{cat}/K_m$ for the lysine peptide is 3-fold higher for R1130E compared to wild type, a 150-fold change in relative substrate specificity. Analysis of the individual steps in the kinetic mechanism using viscosometric techniques indicates that the wild-type enzyme binds the glutamate peptide 3-fold better than the alanine peptide and, at least, 10-fold better than the lysine peptide. For R1130L, this margin range is reduced substantially, and for R1130E, no binding preference is observed. Nonetheless, the lysine peptide binds, at least, 4-fold better to R1130E than to wild type, and the glutamate peptide binds 3-fold poorer to R1130E than to wild type. The mutants lower the phosphoryl transfer rate by 4−30-fold for the three peptides, suggesting that Arg-1130 helps to position the tyrosine for optimum catalysis. The data indicate that a single mutation in v-Fps can alter significantly the relative substrate specificity by about 2 orders of magnitude with, at least, 50% of this effect occurring through relative changes in peptide binding affinity.

The delivery of phosphoryl groups from ATP to specific amino acid side chains in proteins is catalyzed by a large enzyme family known as the protein kinases. The specificity of this exchange and the induced conformational changes in the target upon phosphorylation is the primary biophysical engine for signal transduction. Protein kinases phosphorylate their targets based largely on the immediate residues flanking the site of phosphorylation. Consensus sequences for optimal phosphorylation have been determined using peptide variants in either a manual screening (e.g., refs *2* and *3*) or a random library approach (e.g., refs *4* and *5*). In general, residues that are approximately five residues or less from the phosphorylation site in either the N- or the C-terminal direction are the most significant for directing phosphoryl transfer. The recent X-ray structures for several protein kinases that have been cocrystallized with substrate peptides or inhibitors reveal the sources of their binding specificities. Protein kinases that prefer to phosphorylate positively or negatively charged substrates have the appropriate countercharges in the active site for substrate stabilization. For example, the kinase domain of phosphorylase kinase (PhK)[1] and the catalytic subunit of cAMP-dependent protein kinase (PKA) prefer to phosphorylate substrate peptides with arginine in the P−3 position (*3*).[2] These arginine side chains interact directly with glutamic acid residues in the kinase cores (Glu-110 in PhK and Glu-230 in PKA) (*6*−*8*). In some cases, hydrophobic residues are preferred in the target, and the appropriate hydrophobic pocket is present in the active site to accommodate these side chains. For instance, a phenylalanine in the P−10 position of PKI, the physiological inhibitor for PKA, is essential for high-affinity binding of this protein (*9*). Accordingly, a string of hydrophobic residues in PKA ($Y_{235}$PPFF) form a pocket that recognizes the phenylalanine (*6*).

While there have been X-ray solutions for several tyrosine protein kinases (TPKs) (e.g., refs *10*−*15*), only the kinase domain of the insulin receptor (InRK) has been solved in an active, phosphorylated state with a substrate peptide bound in the active site (*11*). This structure allows an informed glimpse into the recognition elements for tyrosine phospho-

† This work was supported by an NIH grant (CA 75112) and by the California Metabolic Research Foundation.

* To whom correspondence should be addressed. Telephone: (858) 822-3360. Fax: (858) 822-3361. E-mail: joeadams@ucsd.edu.

[1] Abbreviations: GST, glutathione-*S*-transferase; InRK, kinase domain of the insulin receptor; Mops, 3-(*N*-morpholino)propanesulfonic acid; PhK, kinase domain of phosphorylase kinase; PKA, cAMP-dependent protein kinase; TPK, tyrosine-specific protein kinase; v-Fps, nonreceptor TPK and transforming agent of the Fujinami sarcoma virus.

[2] For protein kinases, the site of phosphorylation is called the P-site. All positions N-terminal to the P-site are designated P−1, P−2, P−3, etc., and all positions C-terminal are designated P+1, P+2, P+3, etc.

10.1021/bi992096j CCC: $19.00 
Published on Web 12/11/1999

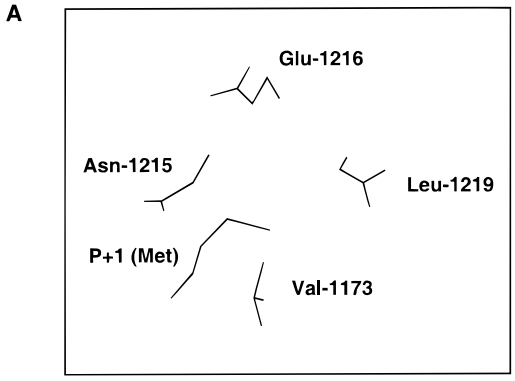


FIGURE 1: (A) Side chains of residues contacting the P+1 methionine in the InRK. The side chain of the P+1 methionine of the peptide substrate makes hydrophobic interactions with Val-1173 and Leu-1219 and the aliphatic portions of Asn-1215 and Glu-1216 (*11*). (B) Sequence alignment of the InRK and v-Fps in regions that form the P+1 pocket of the InRK. The amino acids in the InRK and the residues in v-Fps that comprise the P+1 pocket are underlined. Leu-1219 and the corresponding residue in v-Fps, Arg-1130, are in boldface type.

rylation in this enzyme. InRK prefers to phosphorylate substrate peptides with the following consensus sequence: YMXM, where X is variable (*16*). As shown in Figure 1A, the P+1 methionine inserts into a hydrophobic pocket composed of several side chains. In particular, the side chains of Val-1173 and Leu-1219 and the aliphatic portions of Asn-1215 and Glu-1216 form a hydrophobic pocket that cradles the P+1 methionine. This arrangement of hydrophobic moieties about a P+1 side chain is not unique. In PKA, a kinase that prefers to phosphorylate substrates with hydrophobic residues in the P+1 position, Pro-203 is in the same position as Val-1173 (*6*). Furthermore, the P+1 pocket in PKA contains a cluster of hydrophobic side chains (Leu-198, Pro-203, Leu-205) that can sequester and stabilize a hydrophobic residue.

v-Fps is a nonreceptor TPK, and, as a member of the Fps/Fes family, its cellular forms are predominantly expressed in hematopoietic cells. The Fps/Fes enzymes are essential for the terminal differentiation of macrophages (*17*, *18*), but oncogenic forms have been linked to cardiac disorders in mice (*19*, *20*). v-Fps is an oncogenic form of the cellular enzyme c-Fps, which differs from its normal form by the addition of a retroviral gag sequence at the N-terminus which imparts membrane association. The Fps/Fes family are complex proteins with molecular masses in excess of 90 kDa and are composed of noncatalytic domains that regulate the function of the kinase domain in the absence of receptor signaling. This family is rather unique compared to the widely studied Src family nonreceptor TPKs since the SH2 (Src homology-2) domain activates the kinase domain (*21*) rather than represses it as in the case of c-Src. v-Fps is an ideal model system for the study of protein kinase regulation and catalysis since it is less complex than the Src family TPKs and has been expressed in an active, phosphorylated form in bacteria as GST fusion proteins (*22*). This fusion protein autophosphorylates and readily phosphorylates nine residue substrate peptides with high catalytic efficiency (*23*, *24*).

c-Fps prefers to phosphorylate tyrosine-containing peptides when a glutamic acid is in the P+1 position (*16*). While there is presently no crystallographic structure for a member of the Fps/Fes protein kinase family either with or without a substrate or inhibitor bound, the amino acid sequence of v-Fps suggests that the P+1 pocket of the enzyme may be different than that for the InRK. As shown in Figure 1B, two of the four residues in the P+1 pocket of the InRK (Val-1173 and Asn-1215) are identical in v-Fps (Val-1084 and Asn-1126). Glu-1216 in the InRK is replaced with Gln-1127 in v-Fps, but the aliphatic portion which interacts with the P+1 methionine is retained. In contrast, Leu-1219 is replaced with Arg-1130 in v-Fps, a nonconservative substitution based on charge and size. Given this difference, we wondered whether the unique substrate specificity of v-Fps compared to the InRK could be due to the presence of Arg-1130, a residue that may interact favorably with the P+1 glutamate. To test this hypothesis, we substituted Arg-1130 with leucine (R1130L) and glutamate (R1130E) to see whether the substrate specificity of v-Fps could be altered. We found that the mutations cause up to a 150-fold change in relative substrate specificity. Viscosometric analyses indicate that, at least, 50% of this change in specificity is due to relative changes in substrate binding affinity.

## MATERIALS AND METHODS

*Materials.* Adenosine 5′-triphosphate (ATP), phosphoenolpyruvate, magnesium chloride, nicotinamide adenine dinucleotide, reduced NADH, isopropyl-$\beta$-thiogalactoside (IPTG), tris(hydroxymethyl)aminomethane (Tris), 3-(*N*-morpholino)propanesulfonic acid (Mops), pyruvate kinase, type II, from rabbit muscle, lactate dehydrogenase, type II, from bovine heart, and ethylenediaminetetraacetic acid (EDTA) were purchased from Sigma. Dithiothreitol (DTT) was purchased from Fisher. Media supplies (yeast extract and tryptone) were purchased from Difco. Oligonucleotides were synthesized by Retrogen. DNA mini-prep kits were purchased from Qiagen. The plasmid vector pGEX-2T was purchased from Pharmacia. *E. coli* strain BL21(DE3) was purchased from Novagen. QuikChange kits and *E. coli* strain SURE were purchased from Stratagene.

*Construction of Mutant Proteins.* Mutants in the kinase domain of the v-Fps gene were made by PCR with a MJ Research PCT 200 Peltier Thermocycler, using two oligonucleotides that overlapped at the site of the desired mutation. The following sets of oligonucleotides were used to make the mutations: R1130E, 5′-CAGCAACCAGCAGACGGAAGAGGCCATCGAGCAGC-3′ and 5′-GCTGCTCGATGGCCTCTTCCGTCTGCTGGTTGCTG-3′; R1130L, 5′-AACCAGCAGACGCTCGAGCGGATCGAG-3′ and 5′-GCTCGATGGCCTCGAGCGTCTGCTGGTT-3′. The PCR reactions were performed in a total volume of 50 $\mu$L with 60 mM Tris (pH 9.1), 18 mM $(NH_4)_2SO_4$, 1.8 mM $MgSO_4$, 5−50 ng of template DNA, 0.2 mM of each dNTP, 2.5 units of *PfuTurbo* DNA polymerase, and 125 ng of each primer. The PCR cycle created the mutation in the gene while amplifying the plasmid and gene together. The plasmid was purified and transformed into a recombinant minus strain of *E. coli*. Several clones were selected and their entire kinase genes

sequenced. The mutant plasmids with the correct sequence were then transformed into *E. coli* strain BL21(DE3), and expression of the GST fusion protein was confirmed on a 12% polyacrylamide gel.

*Peptides and Protein Purification.* Substrate peptides, EAEIYEAIE, EAEIYAAIE, and EAEIYKAIE, were synthesized by the USC Microchemical Core Facility using Fmoc chemistry and purified by C-18 reverse phase HPLC. The concentration of the peptides was determined by weight. BL21(DE3) cells containing the mutant or wild-type plasmid were grown to an $OD^{600}$ of approximately 0.8 at 37 °C in 6 L of LB media and induced for 5 h with 1 mM IPTG at 24 °C. The cells were harvested by centrifugation. The wild-type and mutant fusion proteins, GST-kin, were purified using a glutathione agarose affinity resin according to previously published procedures (*22*). The total mass of the eluted protein (approximately 3−4 mg for wild type and mutants) was determined by a Bradford assay, and the concentration of the fusion protein ($M_r \approx 58\,000$) was determined by gel densitometry (*24*, *25*). A portion of the total protein represents breakdown products of the fusion protein since they migrate near the expected molecular weight of free GST (approximately 29 000) and are recognized by GST antibodies (*25*). The enzyme was stored at −70 °C in a buffer containing 50 mM Tris (pH 7.5), 1 mM EDTA, 150 mM NaCl, 1 mM DTT, 10% glycerol. The enzyme was thawed on ice (4 °C) and used immediately for each kinetic study.

*Kinetic Assay.* The enzymatic activities of GST-kin and the mutants were measured spectrophotometrically using a coupled enzyme assay. This assay couples the production of ADP with the oxidation of NADH using pyruvate kinase and lactate dehydrogenase. In general, peptide (0.1−10 mM) was mixed manually with ATP (0.05−2.8 mM), $MgCl_2$ (10−12.8 mM), and GST-kin (50−400 nM) in a 50 $\mu$L (minimum volume) quartz cuvette containing 0.40 mM phosphoenolpyruvate, 0.20 mM NADH, 2 units of lactate dehydrogenase, and 0.5 unit of pyruvate kinase. The total concentration of $MgCl_2$ needed to obtain a desired, free concentration of $Mg^{2+}$ was calculated based on the dissociation constants of 0.0143 mM for Mg-ATP, 5 mM for Mg-PEP, and 19.5 mM for Mg-NADH (*26*). All reactions were measured in a Beckman DU640 spectrophotometer equipped with a microcuvette holder in a buffer containing 100 mM Mops at pH 7.0, in a final volume of 60 $\mu$L at 23 °C. Background reactions in the absence of substrate peptide were performed to correct for ATPase activity. This background did not exceed 10% of the substrate-dependent reaction for wild-type or mutant enzymes. Absorbance changes at 340 nm were collected over a time range of 100−150 s. Less than 10% of the substrate peptide was consumed in each initial velocity measurement. All initial velocities varied linearly with the concentration of the fusion protein.

*Viscosometric Measurements.* The relative solution viscosities ($\eta^{rel}$) of buffers containing glycerol were measured relative to a standard buffer of 100 mM Mops, pH 7.0, at 23 °C, using an Ostwald viscometer (*27*). Each viscosity measurement was carried out using 5.0 mL of buffer containing varying amounts of viscosogen. The amount of time required for each buffer to move through the markings on the viscometer was recorded. The relative viscosity of each buffer was calculated using eq 1:

Table 1: Nine-Residue Substrate Peptides for the Kinase Domain of v-Fps[a]

| sequence | name |
|---|---|
| EAEIY**E**AIE | P+1 (Glu) |
| EAEIY**A**AIE | P+1 (Ala) |
| EAEIY**K**AIE | P+1 (Lys) |

[a] The variable residue in the P+1 position of the parent peptide, EAEIYXAIE, is shown in boldface type.

$$\eta^{rel} = \frac{t\,(\%)}{t} \times \frac{\rho\,(\%)}{\rho} \qquad (1)$$

where $\eta^{rel}$ is the relative solvent viscosity, $t$ (%) and $t$ are the transit times for a given viscous buffer and the standard buffer, respectively, and $\rho$ (%) and $\rho$ are the densities of the viscous and standard buffers, respectively. The following relative solvent viscosities were obtained for the buffers (% viscosogen, $\eta^{rel}$): 35% glycerol, 3.7, 30% glycerol, 3.0; 25% glycerol, 2.6; 20% glycerol, 2.0. All solvent viscosity measurements were performed in triplicate and did not deviate by more than 4% in value.

*Data Analysis.* The steady-state kinetic parameters $V_{max}$, $K_{peptide}$, and $K_{ATP}$ were obtained by plotting the initial reaction velocity versus the total substrate concentration at fixed ATP concentration or the total ATP concentration at fixed peptide concentration using the Michaelis−Menten equation. The maximum reaction velocity ($V_{max}$) was converted to $k_{cat}$ by dividing $V_{max}$ by the total enzyme concentration.

## RESULTS

*Steady-State Kinetic Parameters for Mutant Proteins.* The steady-state kinetic parameters for the mutants and wild type were determined from plots of initial velocity ($v$) versus ATP or substrate peptide concentration using a coupled enzyme assay in 50 mM Mops (pH 7). Plots of $v$ versus peptide concentration (0.1−10 mM) at fixed ATP (2.8 mM) and $MgCl_2$ (12.8 mM) were used to measure $k_{cat}$ and $K_{peptide}$ for wild type, R1130L, and R1130E. Plots of $v$ versus ATP concentration (0.05−1 mM) at 1 mM fixed peptide and 10 mM free $Mg^{2+}$ were used to determine $K_{ATP}$ for wild type, R1130L, and R1130E. The values of $K_{ATP}$ for wild type and the mutants are not affected by increasing the concentrations of peptide (data not shown). A complete listing of all steady-state kinetic parameters is included in Table 2. The $K_{ATP}$ values for R1130E are similar to that for wild type but are higher by about 2-fold for R1130L. The mutants have significant effects on $K_{peptide}$. For P+1(Glu), the mutants *increase* $K_{peptide}$ by 3−4-fold, and for P+1(Lys), the mutants *lower* $K_{peptide}$ by more than 4-fold. In contrast, neither mutation alters the apparent affinity of P+1(Ala). R1130L displays similar $k_{cat}$ values for P+1(Glu) and P+1(Ala) compared to wild type (≤2-fold difference). By comparison, R1130E displays a 12- and 6-fold lower $k_{cat}$ for P+1(Glu) and P+1(Ala), respectively. Since plots of initial velocity versus P+1(Lys) for wild type are linear up to 10 mM (data not shown), only a lower limit on $k_{cat}$ and $K_{peptide}$ could be assigned. Owing to solubility problems with high stock concentrations of P+1(Lys), amounts in excess of 10 mM were not readily attained.

*Viscosity Effects on Kinetic Parameters.* The steady-state kinetic parameters, $k_{cat}$ and $k_{cat}/K_{peptide}$, for wild type and

Table 2: Steady-State Kinetic Parameters for the Mutant Forms of v-Fps[a]

| protein | substrate | $k_{cat}$ ($s^{-1}$) | $K_{peptide}$ (mM) | $k_{cat}/K_{peptide}$ ($mM^{-1}$ $s^{-1}$) | $K_{ATP}$ (mM)[b] |
|---|---|---|---|---|---|
| wild type | P+1(Glu) | 14 ± 1 | 0.35 ± 0.040 | 40 ± 5.4 | 0.25 ± 0.05 |
| | P+1(Ala) | 13 ± 2 | 1.2 ± 0.15 | 11 ± 2.2 | |
| | P+1(Lys) | >2[c] | >10[c] | 0.20 ± 0.03[c] | |
| R1130L | P+1(Glu) | 6.5 ± 1.0 | 1.0 ± 0.30 | 6.5 ± 2.2 | 0.37 ± 0.10 |
| | P+1(Ala) | 8.2 ± 1.8 | 1.3 ± 0.40 | 6.3 ± 2.4 | 0.55 ± 0.12 |
| | P+1(Lys) | 2.0 ± 0.39 | 2.8 ± 1.0 | 0.71 ± 0.29 | 0.50 ± 0.10 |
| R1130E | P+1(Glu) | 1.2 ± 0.20 | 1.5 ± 0.40 | 0.80 ± 0.25 | 0.35 ± 0.03 |
| | P+1(Ala) | 2.2 ± 0.34 | 1.5 ± 0.45 | 1.5 ± 0.51 | 0.31 ± 0.14 |
| | P+1(Lys) | 1.4 ± 0.18 | 2.3 ± 0.70 | 0.61 ± 0.20 | 0.29 ± 0.10 |

[a] The kinetic parameters were measured in 100 mM Mops (pH 7) buffer at 23 °C using the coupled enzyme assay. $k_{cat}$ and $K_{peptide}$ were measured using 2.8 mM ATP and 12.8 mM $MgCl_2$ and varying peptide concentrations (0.2−10 mM). [b] $K_{ATP}$ was measured using fixed concentrations of peptide (1 mM) and 10 mM free $Mg^{2+}$and varying ATP concentrations (0.05−1 mM). [c] Plots of initial velocity versus peptide concentration were linear up to 10 mM so that only lower limits on $k_{cat}$ and $K_{peptide}$ are reported. $k_{cat}/K_{peptide}$ was determined from the slope of the $v$ versus [S] plot.

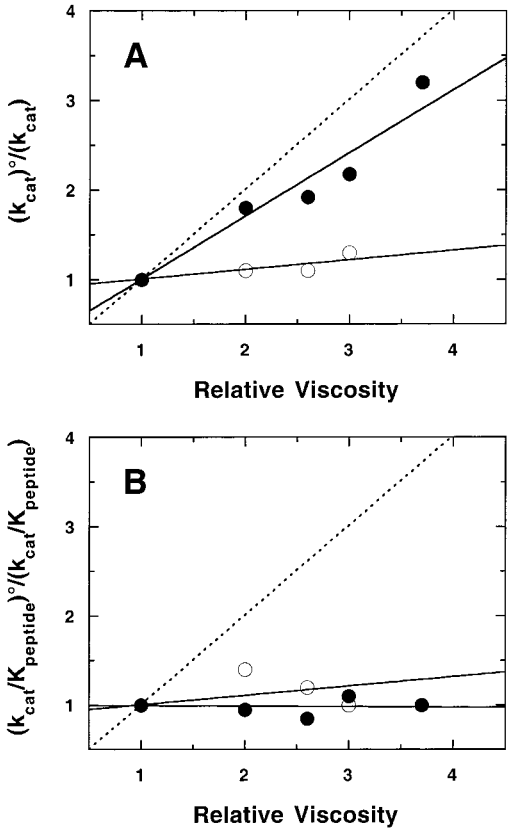


FIGURE 2: Effects of solvent viscosity on the steady-state kinetic parameters for R1130L (○) and the wild-type enzyme (●) using P+1(Glu) as a substrate. (A) Influence of viscosogens on $k_{cat}$. $(k_{cat})^\circ/k_{cat}$ is the ratio of $k_{cat}$ in the absence and presence of varying glycerol concentrations, and $\eta^{rel}$ is the relative solvent viscosity. (B) Influence of viscosogens on $k_{cat}/K_{peptide}$. $(k_{cat}/K_{peptide})^\circ/(k_{cat}/K_{peptide})$ is the ratio of $k_{cat}/K_{peptide}$ in the absence and presence of varying glycerol concentrations, and $\eta^{rel}$ is the relative solvent viscosity. The values of $k_{cat}$ and $k_{cat}/K_{peptide}$ were determined from plots of initial velocity versus substrate peptide concentration (0.1−10 mM) using 2.8 mM ATP and 10 mM free $Mg^{2+}$. The data in both plots were fit to linear functions, and the slope values are reported in Table 3. The dotted lines represent slopes of 1 where the *y*-intercept is the origin.

mutants were measured as a function of varying solvent viscosity using the substrate peptides in Table 1. Plots of $v$ versus peptide concentration (0.1−10 mM) at fixed ATP (2.8 mM) and $MgCl_2$ (12.8 mM) were used to measure $k_{cat}$ and $k_{cat}/K_{peptide}$ for wild type, R1130L, and R1130E at 0, 20, 25, 30, and 35% glycerol. The ratios of these kinetic parameters

Scheme 1

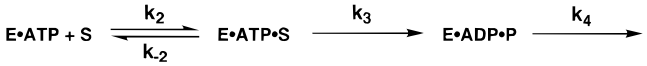


in the absence (superpostscript "°") and presence (no postscript) of glycerol $[(k_{cat})^\circ/(k_{cat})$ and $(k_{cat}/K_{peptide})^\circ/(k_{cat}/K_{peptide})]$ for wild type and R1130L using P+1(Glu) are plotted as a function of relative solvent viscosity in Figure 2. The data were fit to linear functions, and the slopes of these lines $[(k_{cat})^\eta$ and $(k_{cat}/K_{peptide})^\eta]$ are listed in Table 3. Viscosity experiments were also performed on wild type and the mutants using P+1(Glu), P+1(Ala), and P+1(Lys). These data were fit to linear functions, and the slopes are presented in Table 3. The steady-state kinetic parameters for wild-type and mutant proteins at each viscosity value were always measured alongside a 0% glycerol control to compensate for any minor changes in enzyme specific activity on different days. For all enzymes and substrates, the slope values fall between −0.15 and 0.70. With one exception [R1130E and P+1(Ala)], all the values for $(k_{cat})^\eta$ are less than that for wild type using P+1(Glu) or P+1(Ala). A negative slope was obtained for $(k_{cat})^\eta$ for R1130L using P+1(Lys), but this value is indistinguishable from zero given the error in the measurement. In all cases, glycerol had little effect on $k_{cat}/K_{peptide}$ so that the slope values for this parameter are close to zero. In some cases, $(k_{cat}/K_{peptide})^\eta$ is negative, but the error in the measurement does not permit an exact assignment of the value. For all data sets, linear responses between initial velocity and enzyme concentration were obtained, indicating that the coupling reagents are not affected by the viscous media (data not shown).

The viscosometric data shown in Figure 2 and Table 3 can be interpreted according to the simple three-step mechanism shown in Scheme 1. By applying the Stokes−Einstein relationship which equates diffusion coefficients and intrinsic viscosity, a direct correlation between the steady-state kinetic parameters, $k_{cat}$ and $k_{cat}/K_{peptide}$, and the relative solvent viscosity of the medium can be made. Plots of either kinetic parameter as a ratio in the absence and presence of viscosogen versus relative solvent viscosity are linear in most cases (Figure 2), and the slope values conform to eqs 2 and 3:

$$(k_{cat})^\eta = \frac{k_3}{k_3 + k_4} \qquad (2)$$

Table 3: Effects of Solvent Viscosity on the Kinetic Parameters of Mutant Forms of v-Fps[a]

| protein | substrate | $(k_{cat})^{\eta}$ [b] | $(k_{cat}/K_{peptide})^{\eta}$ [b] | $k_3$ ($s^{-1}$)[c] | $k_4$ ($s^{-1}$)[c] | $K_d$ (mM)[d] |
|---|---|---|---|---|---|---|
| wild type | P+1(Glu) | 0.70 ± 0.10 | 0.05 ± 0.10 | 47 ± 16 | 20 ± 3.2 | 1.1 ± 0.40 |
| | P+1(Ala) | 0.64 ± 0.07 | −0.09 ± 0.08 | 36 ± 9.0 | 20 ± 3.8 | 3.3 ± 0.69 |
| | P+1(Lys) | | | >2[e] | | >10[e] |
| R1130L | P+1(Glu) | 0.15 ± 0.05 | 0.11 ± 0.05 | 7.6 ± 1.3 | 43 ± 16 | 1.0 ± 0.08 |
| | P+1(Ala) | 0.33 ± 0.05 | −0.01 ± 0.03 | 12 ± 2.8 | 25 ± 6.6 | 1.9 ± 0.15 |
| | P+1(Lys) | −0.15 ± 0.20 | 0.10 ± 0.15 | 2 | ≥20 | 2.5 ± 0.65 |
| R1130E | P+1(Glu) | 0.51 ± 0.10 | −0.11 ± 0.07 | 2.4 ± 0.63 | 2.4 ± 0.62 | 3.1 ± 0.67 |
| | P+1(Ala) | 0.63 ± 0.09 | −0.10 ± 0.09 | 6.0 ± 1.7 | 3.5 ± 0.74 | 4.0 ± 1.0 |
| | P+1(Lys) | 0.20 ± 0.05 | 0.04 ± 0.09 | 1.6 ± 0.24 | 6.5 ± 1.8 | 2.8 ± 0.32 |

[a] All kinetic parameters were measured in 100 mM Mops (pH 7) buffer at 23 °C using 10 mM free $Mg^{2+}$. [b] $(k_{cat})^{\eta}$ and $(k_{cat}/K_{peptide})^{\eta}$ are the slope values for plots of the steady-state kinetic parameters as ratios in the absence and presence of glycerol versus the relative solvent viscosities. These effects were measured from $v$ vs substrate concentration (0.1−6 mM) plots at fixed concentrations of ATP (2.8 mM). [c] The values of $k_3$ and $k_4$ were derived from the expression for the turnover number $[k_3k_4/(k_3 + k_4)]$ and $(k_{cat})^{\eta}$ by the following relationships: $k_4 = k_{cat}/(k_{cat})^{\eta}$ and $k_3 = k_{cat}/[1 - (k_{cat})^{\eta}]$. [d] The $K_d$ values for the peptide were measured using eq 4. Negative values of $(k_{cat})^{\eta}$ and $(k_{cat}/K_{peptide})^{\eta}$ were treated as zero. [e] The values of $k_3$ and $K_d$ were estimated from the steady-state kinetic parameters in Table 2 and not from viscosity data.

$$(k_{cat}/K_{peptide})^{\eta} = \frac{k_3}{k_{-2} + k_3} \quad (3)$$

Equations 2 and 3 predict that the slope values will fall between the limits of 0 and 1 where the former represents a viscosity-insensitive parameter and the latter represents a viscosity-sensitive parameter. In some cases (e.g., Figure 2B, R1130L), the data for $k_{cat}/K_{peptide}$ display some scatter, but this occurs only when the parameter is mostly viscosity-insensitive and $(k_{cat}/K_{peptide})^{\eta}$ approximates zero. As shown in Table 3, these slope values fall between the expected limits given the measurement errors. We can use the rate expressions for $k_{cat}$ $[k_3k_4/(k_3 + k_4)]$ and $k_{cat}/K_{peptide}$ $[k_2k_3/(k_{-2} + k_3)]$ and eqs 2 and 3 to determine the individual steps in Scheme 1. In addition, the dissociation constants for the substrate peptides can be estimated using eq 4.

$$K_d = \frac{K_{peptide}[1 - (k_{cat}K_{peptide})^{\eta}]}{[1 - (k_{cat})^{\eta}]} \quad (4)$$

By applying this approach to wild-type v-Fps and the mutants, the individual steps in the kinetic mechanism can be assigned (Table 3).

## DISCUSSION

Protein kinases phosphorylate the correct substrates based, in part, on the local sequence elements flanking the site of phosphorylation (*3*). For the nonreceptor TPK, c-Fps, the optimal peptide EEEIYEEIE was generated from a random peptide library search, but the P−1 and P+1 positions were identified as the primary determinants for efficient catalysis (*16*). This peptide is an excellent substrate for the kinase domain of v-Fps, as well, displaying a turnover number similar to that for PKA and its best substrates (*23*, *24*). Based on the relatedness of the kinase domains in the Fps/Fes enzyme family, it is likely that the specificity of v-Fps is similar to that for c-Fps. In support of this claim, replacement of the P−1 isoleucine with alanine causes an 8-fold drop in $k_{cat}/K_{peptide}$ (*23*), in keeping with the library search for c-Fps (*16*). Replacement of the P−3 and P+2 glutamates with alanine (EAEIYEAIE) results in no changes in the steady-state kinetic parameters for v-Fps (*24*). Furthermore, replacement of the P−4, P−2, P+1, and P+4 glutamates with aspartate (DADIYDAID) leads to no changes in the kinetic parameters (*24*). Again, these findings are consistent with the library search which predicts that residues outside the P+1 and P−1 positions will play a diminished role in determining substrate specificity (*16*).

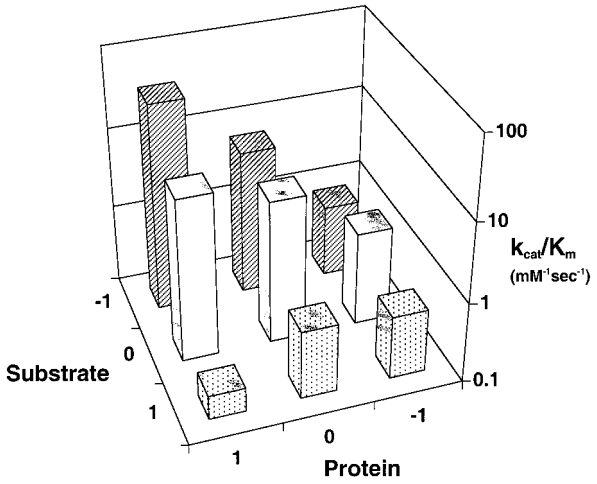


FIGURE 3: Effects of mutations on $k_{cat}/K_{peptide}$ for P+1(Glu), P+1(Ala), and P+1(Lys). The three enzyme forms are designated on the protein axis as 1, 0, and −1 for wild type, R1130L, and R1130E, respectively. The three peptide forms are designated on the substrate axis as −1, 0, and 1 for P+1(Glu), P+1(Ala), and P+1(Lys), respectively. The values of $k_{cat}/K_{peptide}$ for P+1(Glu), P+1(Ala), and P+1(Lys) are displayed in the striped, open, and dotted bars, respectively.

*Effects of Mutations on the Steady-State Kinetic Parameters.* To investigate the importance of the P+1 position for controlling the substrate specificity of v-Fps, the steady-state kinetic parameters for the kinase domain were measured using three peptides that differ by substitutions in the P+1 position (Table 1). The kinetic parameters were measured for these substrates using wild-type v-Fps and two mutants that substitute Arg-1130 for leucine (R1130L) or glutamate (R1130E) in the putative P+1 pocket of the enzyme (Figure 1). The desired effect is to generate three enzyme forms and three substrates that differ by charge. As shown in Table 2, the steady-state kinetic parameters vary considerably within the enzyme and peptide series. As shown in Figure 3, $k_{cat}/K_{peptide}$ varies greatly within the peptide and enzyme series. In this plot, the *x*- and *y*-axes display the substrate and enzyme charges assuming that the relevant amino acids (i.e.,

the P+1 position in the peptide or the 1130 position in the protein) adopt ionization states predicted by their solvent p$K_a$ values at neutral pH. As shown in Figure 3, $k_{cat}/K_{peptide}$ for P+1(Glu) is reduced by 6- and 50-fold for R1130L and R1130E compared to the wild-type enzyme (striped bars). These data indicate that a progressive charge change in the putative P+1 pocket from $+1 \Rightarrow 0 \Rightarrow -1$ causes a reduction in preference for the negatively charged peptide variant, P+1-(Glu). This is expected based on an electrostatic consideration of the putative P+1 pocket and peptide position. This trend is also observed for P+1(Ala) although the magnitude of the relative change is considerably reduced, an outcome expected from reduced charge−charge interactions. Finally, an inverse trend in specificity is observed for the lysine peptide. For P+1(Lys), $k_{cat}/K_{peptide}$ is increased by approximately 3-fold for both R1130L and R1130E compared to the wild-type enzyme (dotted bars). This observation is consistent with an electrostatic model for the putative P+1 pocket, but the magnitude of the effect is small compared to that seen for P+1(Glu) in the same enzyme series (i.e., wild type $\Rightarrow$ R1130L $\Rightarrow$ R1130E). Overall, the $k_{cat}/K_{peptide}$ data follow simple electrostatic predictions although other factors must be involved in governing the substrate specificity of v-Fps.

The data displayed in Figure 3 demonstrate how the relative substrate specificity of v-Fps changes for each peptide within a given enzyme series (i.e., same coded bars). A comparison of each enzyme form within a given peptide series also provides unique insights into these specificity changes. Based on $k_{cat}/K_{peptide}$, wild-type v-Fps prefers to phosphorylate P+1(Glu) over P+1(Ala) and P+1(Lys) by 4- and 200-fold. These are large changes in specificity that are consistent with electrostatic complementary in the putative P+1 pocket (Figure 1). For R1130L, this range of effects is truncated dramatically, and for R1130E, all peptides are phosphorylated with similar rate constants. This result is not predicted from a simple electrostatic consideration of the mutants and substrates and suggests that other compensating effects are at work. Nonetheless, comparison of the $k_{cat}/K_{peptide}$ data in Figure 3 indicates that the general trend in the data across the enzyme and peptide series is consistent with a direct role for Arg-1130 in controlling substrate specificity. Overall, insertion of a glutamic acid in place of an arginine in the putative P+1 pocket causes a 50-fold reduction in the ability to phosphorylate a peptide containing a P+1 glutamate and leads to a 3-fold increase in the ability to phosphorylate a peptide containing a P+1 lysine. This amounts to an overall relative specificity change of 150-fold in v-Fps by a single amino acid substitution.

*Peptide Binding Effects.* Steady-state kinetic measurements are useful for comparing the catalytic efficiencies of an enzyme for different substrates. However, these parameters alone do not provide a mechanistic source of the specificity changes in Figure 3. To gain further insights into the kinetic mechanism of v-Fps and its mutant forms, we measured the individual steps in the kinetic mechanism using a viscosometric approach. This approach has been used earlier to determine kinetic mechanisms for wild-type and mutant forms of v-Fps (*1*, *23*−*25*) and PKA (*28*−*31*). It has been shown previously that, for wild-type v-Fps and P+1(Glu), the enzyme−ATP binary complex binds the substrate with moderate affinity ($k_{-2}/k_2 \approx 1$ mM and $k_3 \ll k_{-2}$) to form the central complex (E·ATP·S) and turnover is partially controlled by the rate of phosphoryl transfer ($k_3 = 40$ s$^{-1}$) and net product release ($k_4 = 20$ s$^{-1}$) (*24*). As shown in Table 3, similar kinetic parameters were measured for this preparation of wild-type v-Fps.

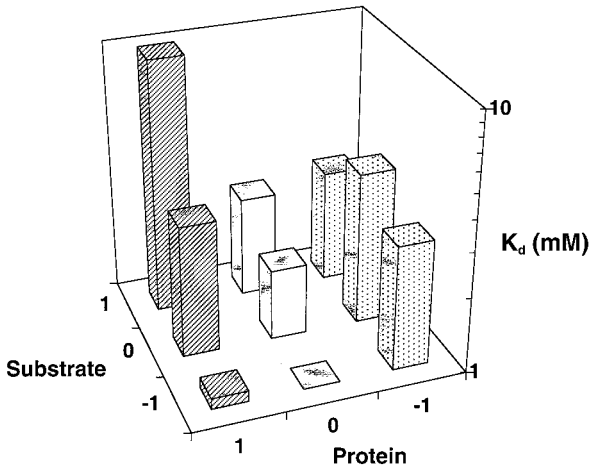


FIGURE 4: Effects of Mutations on $K_d$ for P+1(Glu), P+1(Ala), and P+1(Lys). The three enzyme forms are designated on the protein axis as 1, 0, and −1 for wild type, R1130L, and R1130E, respectively. The three peptide forms are designated on the substrate axis as −1, 0, and 1 for P+1(Glu), P+1(Ala), and P+1(Lys), respectively. The values of $K_d$ for wild type, R1130L, and R1130E are displayed in the striped, open, and dotted bars, respectively.

A salient feature of the viscosity approach is that dissociation constants for substrate peptides can be determined using eq 4. The $K_d$ values for the three peptides are presented in Table 3 for the enzymes and are displayed in the bar diagram in Figure 4 for more direct comparison. P+1(Glu) binds 3- and, at least, 10-fold better to the wild-type enzyme than P+1(Ala) and P+1(Lys) (striped bars). For P+1(Lys), only a lower limit of 10 mM can be placed on $K_d$ using eq 4.[3] This binding trend is predicted based on the charge changes in the P+1 position of the peptide and its expected interaction with Arg-1130 (Figure 1). Replacement of this residue with leucine (R1130L) limits significantly the range of these effects (open bars), and, for R1130E, all three peptides bind equally well (dotted bars). While it reasonable to expect that R1130L might be insensitive to the nature of the P+1 position of the peptide, the absence of a peptide response to R1130E suggests that other factors are important for peptide recognition. For example, inappropriate orientation of the two side chains in the P+1(Lys):R1130E pair or other neighboring residue effects in the mutant may overcome the expected enhancement from the $\epsilon$-amino group. Whatever the cause, the data clearly indicate that Arg-1130 is interacting with the glutamate in the P+1 position of the substrate since replacement of this residue with glutamic acid leads to a 3-fold or more enhancement in the affinity of P+1-(Lys) and a 3-fold reduction in the affinity of P+1(Glu).

Since the peptides in Table 1 exchange rapidly with wild type and mutants based on viscosity measurements (Table 3), the catalytic efficiency of the enzymes, $k_{cat}/K_{peptide}$, is related to the ratio of the rate of phosphoryl transfer and the

[3] Although viscosity measurements could not be made on P+1(Lys) with wild-type v-Fps, we presume that this substrate is in rapid exchange with the enzyme since the other peptides have low values for $(k_{cat}/K_{peptide})^{\eta}$ and $K_{peptide}$ is high (Table 2).

dissociation constant of the peptide (i.e., $k_{cat}/K_{peptide} = k_3/K_d$). As shown in Figures 3 and 4, the changes in $k_{cat}/K_{peptide}$ for the enzymes follow the observed changes in $K_d$. The 4- and 200-fold reductions in $k_{cat}/K_{peptide}$ for P+1(Ala) and P+1(Lys) compared to P+1(Glu) for wild type are reflected in a 3- and, more than, 10-fold decrease in peptide binding affinity for these peptides. The entire change in substrate specificity for P+1(Ala) compared to P+1(Glu) is due to changes in binding affinity with no changes in phosphoryl transfer (Table 3). Since only a lower limit on the $K_d$ for P+1(Lys) could be measured, only a portion of the specificity change for this peptide could be attributed to binding effects. However, this contribution (approximately 50%) is a lower limit so that it is possible that a larger portion of the specificity change could be due to changes in peptide binding affinity. For R1130L, there are no changes in $k_{cat}/K_{peptide}$ for P+1(Glu) and P+1(Ala) (Table 3), and, likewise, there are no significant changes in peptide affinity (Figure 4). In contrast, the 9-fold drop in substrate specificity for P+1(Lys), compared to P+1(Glu) for this mutant, is accounted for partly by a 2-fold increase in peptide $K_d$ (Figure 4), implying that ground state interactions in this peptide−enzyme complex justify approximately 25% of the observed specificity change. For R1130E, there are no notable changes in peptide binding affinity and no significant changes in substrate specificity within the peptide series (Figures 3 and 4). Overall, the progressive disappearance of substrate specificity within the peptide series (striped ⟹ open ⟹ dotted bars in Figure 3) follows the trends in peptide binding affinities (same coded bars in Figure 4).

*Effects on Phosphoryl Transfer*. While the relative changes in peptide affinities (Figure 4) correlate with the relative changes in substrate specificities (Figure 3), the absolute changes in affinities do not account for the absolute changes in substrate specificities in all cases (see previous section). These observations imply that changes in the rates of phosphoryl transfer are also important for understanding the effects of the mutants. As shown in Table 3, for wild type, there is no change in $k_3$ for P+1(Glu) and P+1(Ala), and the value for P+1(Lys) is indeterminate. The absence of an effect in the former case may indicate that the negative charge in P+1(Glu) may have no influence on the "in flight" phosphoryl group, but the reduced binding affinity of P+1(Ala) compared to P+1(Glu) suggests that there are differences in the stability of the two peptides in the active site. The absence of large relative effects on phosphoryl transfer for the glutamate and alanine peptides in both mutants (i.e., ≤2-fold) suggest that this is a general phenomenon for the enzymes (Table 3). In comparison, the rate of phosphoryl transfer to P+1(Lys) is slower than that for P+1(Glu) and P+1(Ala) for R1130L by 4−6-fold. For R1130E, the rate of phosphoryl transfer for P+1(Lys) is similar to that for P+1(Glu) but lower than that for P+1(Ala) by approximately 4-fold. While it is difficult to rationalize these effects within the peptide series, in general, the mutants deliver the phosphoryl group from ATP at rates that are 6−29-fold lower for all peptides compared to wild type and P+1(Glu). These effects are significant and can account for some of the absolute specificity changes within the enzyme series. For example, the reduction in $k_{cat}/K_{peptide}$ for P+1(Glu) upon replacement of Arg-1130 with glutamate is due to a 20-fold reduction in $k_3$ with only a 3-fold reduction in peptide binding affinity (Table 3). For P+1(Ala) and R1130E, the 7-fold reduction in $k_{cat}/K_{peptide}$ compared to this peptide and wild type is due entirely to changes in $k_3$ (Table 3). Despite these changes, for P+1(Lys), the 3-fold increase in $k_{cat}/K_{peptide}$ for R1130E compared to wild type may be explained entirely by changes in $K_d$.

*A Multifunctional P+1 Pocket.* Three observations indicate that Arg-1130 interacts directly with residues in the P+1 position of substrate peptides. First, P+1(Lys) binds, at least, 4-fold better to R1130E than to wild type (Table 3). Second, P+1(Glu) binds 3-fold better to wild type than to R1130E (Table 3). Third, the mutations do not affect ATP affinity (Table 2), suggesting that Arg-1130 does not interact with the nucleotide and the mutations do not have global effects on structure. $K_{ATP}$ values for R1130E and wild type are similar. Although $K_{ATP}$ values for R1130L are larger than wild type by approximately 2-fold, the predicted $K_d$ values are similar (Table 3).[4] While it is difficult to rationalize these observations and the relative specificity changes in Figure 3 without a vicinal Arg-1130 in the P+1 pocket, the data presented herein suggest that recognition of substrates via this pocket does not rest solely on charge−charge interactions. As shown in Figure 4, R1130E is not sensitive to the charge in the P+1 peptide position as expected. A portion of this effect may be due to subtle conformational changes that alter residues in the pocket. If this region in v-Fps is similar to that in the InRK (Figure 1), several hydrophobic contributions may stabilize the peptide side chain. Whatever the cause, the changes in peptide affinity for the mutants can be explained partly through charge−charge interactions, but certainly others factors such as van der Waals contacts participate in the P+1 pocket of v-Fps. In this way, the P+1 pocket of v-Fps, unlike that for the InRK or PKA, may be multifunctional, taking advantage of both charge and hydrophobic contacts with the substrate. These characteristics of the pocket may also explain why v-Fps and its family members phosphorylate tyrosine residues with carboxylate or noncharged residues in the P+1 position although the former is preferred.

[4] Equation 4 can be used to predict the true affinities of ATP for wild type and mutants assuming that $(k_{cat}/K_{ATP})^{\eta}$ which replaces $(k_{cat}/K_{peptide})^{\eta}$ is 0, an observation made previously for the wild-type enzyme (*1*). This analysis provides a $K_d$ of 0.83 mM for wild type using P+1(Glu). Similar affinities are estimated for R1130E using P+1(Glu) and P+1(Ala) and for R1130L using P+1(Ala). For R1130E and P+1(Lys) and for R1130L and P+1(Glu) and P+1(Lys), the $K_d$ values are approximately 2-fold lower, but the errors in these measurements are large given the error in $K_{ATP}$ (Table 2).

## REFERENCES

1. Saylor, P., Wang, C., Hirai, T. J., and Adams, J. A. (1998) *Biochemistry 37*, 12624−12630.
2. Kemp, B. E., and Pearson, R. B. (1991) in *Protein Phosphorylation (Part A)* (Hunter, T., and Sefton, B. M., Eds.) pp 121−134, Academic Press, Inc., San Diego.
3. Pearson, R. B., and Kemp, B. E. (1991) *Methods Enzymol. 200*, 62−81.
4. Songyang, Z., Blechner, S., Hoagland, N., Hoekstra, M. F., Piwnica-Worms, H., and Cantley, L. C. (1994) *Curr. Biol. 4*, 973−981.
5. Lam, K. S. (1998) *Methods Mol. Biol. 87*, 83−86.
6. Knighton, D. R., Zheng, J., Ten Eyck, L. F., Xuong, N.-h., Taylor, S. S., and Sowadski, J. M. (1991) *Science 253*, 414−420.

7. Knighton, D. R., Bell, S. M., Zheng, J., Ten Eyck, L. F., Xuong, N.-h., Taylor, S. S., and Sowadski, J. M. (1993) *Acta Crystallogr. D49*, 357−361.
8. Lowe, E. D., Noble, M. E. M., Skamnaki, V. T., Oikonomakos, N. G., Owen, D. J., and Johnson, L. N. (1997) *EMBO J. 16*, 6646−6658.
9. Glass, D. B., Lundquist, L. J., Katz, B. M., and Walsh, D. A. (1989) *J. Biol. Chem. 264*, 14579−14584.
10. Hubbard, S. R., Mohammadi, M., and Schlessinger, J. (1998) *J. Biol. Chem. 273*, 11987−11990.
11. Hubbard, S. R. (1997) *EMBO J. 16*, 5572−5581.
12. Sicheri, F., Moarefi, I., and Kuriyan, J. (1997) *Nature 385*, 602−609.
13. Xu, W., Harrison, S. C., and Eck, M. J. (1997) *Nature 385*, 595−602.
14. Hubbard, S. R., Wei, L., Ellis, L., and Hendrickson, W. A. (1994) *Nature 372*, 746−754.
15. Yamaguchi, H., and Hendrickson, W. A. (1996) *Nature 384*, 484−489.
16. Songyang, Z., Carraway, K. L., Eck, M. J., Feldman, R. A., Mohammadl, M., Schlessinger, J., Hubbard, S. R., Smith, D. P., Eng, C., Lorenzo, M. J., Ponder, B. A. J., Mayer, B. J., and Cantley, L. C. (1995) *Nature 373*, 536−539.
17. MacDonald, I., Levy, J., and Pawson, T. (1985) *Mol. Cell. Biol. 5*, 2543−2551.
18. Feldman, R. A., Gabrilove, J. L., Tam, J. P., Moore, A. S., and Hanafusa, H. (1985) *Proc. Natl. Acad. Sci. U.S.A. 82*, 2379−2383.
19. Yee, S.-P., Mock, D., Greer, P., Maltby, V., Rossant, J., Bernstein, A., and Pawson, T. (1989) *Mol. Cell. Biol. 9*, 5491−5499.
20. Yee, S.-P., Mock, D., Maltby, V., Silver, M., Rossant, J., Bernstein, A., and Pawson, T. (1989) *Proc. Natl. Acad. Sci. U.S.A. 86*, 5873−5877.
21. Koch, C. A., Moran, M., Sadowski, I., and Pawson, T. (1989) *Mol. Cell. Biol. 9*, 4131−4140.
22. Gish, G., McGlone, M. L., Pawson, T., and Adams, J. A. (1995) *Protein Eng. 8*, 609−614.
23. Adams, J. A. (1996) *Biochemistry 35*, 10949−10956.
24. Wang, C., Lee, T. R., Lawrence, D. S., and Adams, J. A. (1996) *Biochemistry 35*, 1533−1539.
25. Saylor, P., Hanna, E., and Adams, J. A. (1998) *Biochemistry 37*, 17875−17881.
26. Martell, A. E., and Smith, R. M. (1977) *Critical Stability Constants*, Vol. 3, Plenum, New York.
27. Shoemaker, D. P., and Garland, C. W. (1962) *Experiments in Physical Chemistry*, 2nd ed., McGraw-Hill, New York.
28. Adams, J. A., and Taylor, S. S. (1993) *Protein Sci. 2*, 2177−2186.
29. Adams, J. A., and Taylor, S. S. (1992) *Biochemistry 31*, 8516−8522.
30. Grant, B. D., Hemmer, W., Tsigelny, I., Adams, J. A., and Taylor, S. S. (1998) *Biochemistry 37*, 7708−7715.
31. Grant, B. D., Tsigelny, I., Adams, J. A., and Taylor, S. S. (1996) *Protein Sci. 5*, 1316−1324.

BI992096J